9420 J. Phys. Chem. A **1998,** *102,* 9420−9426

Cluster Impact Chemistry

Wolfgang Christen* and Uzi Even

School of Chemistry, Tel Aviv University, Tel Aviv 69978, Israel

Received: April 15, 1998; In Final Form: August 5, 1998

This paper addresses the interaction of molecular cluster ions with a solid surface in the kinetic energy range of 1−100 eV/molecule. We report experimental results on the energy acquisition by the cluster following its impact on the target, the size distribution and the time scale of cluster fragmentation, and first examples of chemical reactions induced by cluster impact. In particular we show that for a *p*-type diamond film and moderate collision energies the elasticity of the cluster-surface impact is surprisingly high: The intact cluster recoils with typically 75% of its collision energy. Once, however, the clusters have acquired sufficient internal energy they will shatter, mostly to monomers. In the case of protonated ammonia cluster ions this shattering of clusters upon surface impact is shown to be faster than 80 ps. It provides evidence that the technique of cluster impact allows an ultrafast energy redistribution within superheated cluster ions prior to their fragmentation. The feasibility of this fascinating new approach to femtosecond chemistry is demonstrated with impact-induced chemical reactions of iodomethane clusters to molecular iodine and of trifluoromethane clusters to molecular fluorine. The detected reaction yields are surprisingly high, even for the small cluster sizes investigated so far ($n < 16$).

1. Introduction

While cluster science has grown to a well-established field during the last decades, recently a new and potentially useful area has emerged, i.e., the investigation of phenomena involving the interaction of clusters with solid surfaces. Experimental results for the scattering of atomic and molecular clusters from solid surfaces have been reported for neutral[1−31] and ionic[32−60] clusters, as well as secondary electron emission due to the impact of clusters,[52,61−78] for a large variety of clean or adsorbate-covered, polycrystalline or single-crystal surfaces.

Whereas detailed information about cluster properties in the gas phase and surface scattering of C_{60} and its derivatives[39,79−110] has been obtained, little is known about the interaction process of clusters with solid surfaces at hyperthermal energies.

The net result of these investigations is the observation of cluster fragmentation upon surface impact. With increasing kinetic energy of the clusters, their fragmentation, neutralization, and adsorption on the target surface in general increases. Under certain circumstances even the emission of electrons and the dissociation or the ionization of the clusters can be observed, which possibly could be explained by an energy localization within the cluster and the substrate. Another mechanism for the dissipation of the initial kinetic energy, besides target excitation, is the conversion to vibrational excitation, especially in the case of C_{60}.

In this paper we will address the inelastic interaction of ion clusters with solid surfaces in the kinetic energy range of 1−100 eV/molecule, aiming at collision-induced cluster-specific chemical reactions. The experimental method is presented in section 2, while in section 3 the results will be reported and discussed: The fragment size distribution of clusters following their impact on the target is addressed in section 3.1, the time scale of cluster fragmentation in section 3.2, the transfer of kinetic energy of the clusters to the target in section 3.3, collision-induced cluster dissociation in section 3.4, and first examples of cluster impact chemistry in section 3.5.

2. Experimental Setup

The basic setup of the experimental apparatus has been described in detail elsewhere.[59] Here we give only a brief description of the features relevant to the present study.

The instrument used for our investigations consists mainly of a cluster ion source, a primary time-of-flight mass spectrometer, an ion mirror, and an ultrahigh vacuum target collision chamber containing a secondary time-of-flight mass spectrometer.

Cluster ions are efficiently generated by supersonic expansion of the gaseous substance diluted with a carrier gas and subsequent ionization by electrons emitted from a pulsed filament. The expanding jet is collimated and passed to the primary time-of-flight mass spectrometer, where ions are extracted perpendicular to the axis of the neutral beam and are accelerated to a kinetic energy of about 2000 eV. Mass selection of the beam is achieved by pulsing the high voltage applied at a planar ion mirror, at the correct timing, deflecting a single cluster size by 90° into the scattering chamber (about 10^6 ions/pulse). Incident cluster ions are perpendicular to a silicon target, which is coated with a $\simeq 10\ \mu$m thick *p*-type diamond film[111] and heated to about 400 K. Cluster ions are decelerated to the desired collision energy by using a strong retarding field between a grounded mesh and the target surface, to which a high voltage is applied. The same high field that decelerates the incoming cluster ions is also used to efficiently collect and reaccelerate scattered ions. It allows a mass analysis of fragment ions through their time-of-flight from the target to the detector. This second time-of-flight mass spectrometer is equipped with a retarding field energy analyzer in front of the ion detector to determine the kinetic energy distribution of ions.

This measurement is accomplished by a mass-specific integration of transmitted ions as a function of the retarding voltage of the analyzer. As has been shown previously,[59] the measured data can be fitted nicely to an error function, which corresponds to a Gaussian energy distribution of the beam. The

10.1021/jp981874z CCC: $15.00

Gaussian maximum is taken as the mean kinetic energy of the ions. The energy spread of the primary cluster beam is less than 1% of the kinetic energy.

Two unique features of the experimental setup should be emphasized: The first is a design where the angle of incidence is always normal to the target surface for all ions, contrary to most scattering experiments using a reflectron collider.[39,44] This setup avoids the complication of a collision-dependent angle of incidence and the errors caused by disregarding the parallel component of the ion energy. The second and more important aspect is the extremely short deceleration region of 0.2−2.0 mm, corresponding to an electric field of up to 10^7 V m^{-1}. This value is more than 30 times stronger than in a typical reflectron-type mass spectrometer. Thus, in contrast to angle-resolved scattering experiments,[86,106] problems of low-energetic ion beams are eliminated and the collection efficiency of charged collision products is maximized. Using SIMION[112] trajectory simulations, we verified that all ions leaving the target with a kinetic energy of less than 100 eV parallel to the target surface can be collected. This feature is highly relevant for two reasons: First, it is known from theory[113−116] and experiment[3,10,16,25] that clusters scatter into large angles with respect to the surface normal and thus can escape collection and detection. Second, it allows us to investigate the important low-energy range of collision energies down to 1 eV without significant loss in ion transmission.

3. Results and Discussion

3.1. Size Distribution of Charged Cluster Fragments. Applying a voltage U_{target} to the target that is higher than the kinetic energy of the incident ions causes the cluster ions to be reflected elastically; that is, without impacting the target. To initiate collisions of cluster ions with the scattering surface, the voltage applied to the target has to be lower than the beam energy. Thus, the collision energy E_{col} is given by the difference between the mean kinetic energy of the impinging ions E_{i} and the target potential U_{target}, $E_{\text{col}} = E_{\text{i}} - eU_{\text{target}}$, e being the elementary charge; negative collision energies E_{col} mean reflection.

Figure 1a shows the fragmentation pattern of protonated clusters of 16 water molecules as a function of the collision energy E_{col}. At very low impact energies $E_{\text{col}} \simeq 0$ eV most of the impinging $(H_2O)_{16}H^+$ cluster ions recoil intact from the target surface. For slightly higher collision energies only few intact parent cluster ions are left, with the simultaneous observation of small ionic fragments, $(H_2O)_nH^+$, $n = 1-4$. No other charged species are detected. As the collision energy is increased, the fragment ion size decreases. The large dip in the total ion yield for impact energies of $E_{\text{col}} = 0-10$ eV could be attributed to efficient neutralization of slow ions on the conducting target.

As a general result, for all the cluster substances and cluster sizes investigated, the fragment ions are small, typically monomers. Especially neither cluster ions that lost one or two subunits nor intermediate-size fragment ions are detected. Obviously there is a pronounced transition from the largely intact rebounding cluster ion to a regime where the cluster disintegrates. However, it should be borne in mind that in the present experimental setup only positively charged ions are measured, and only fragmentation that is faster than the reacceleration time t can be detected directly. This time window is given by

$$t = d\left(\frac{m}{2eU_{\text{target}}}\right)^{1/2}$$

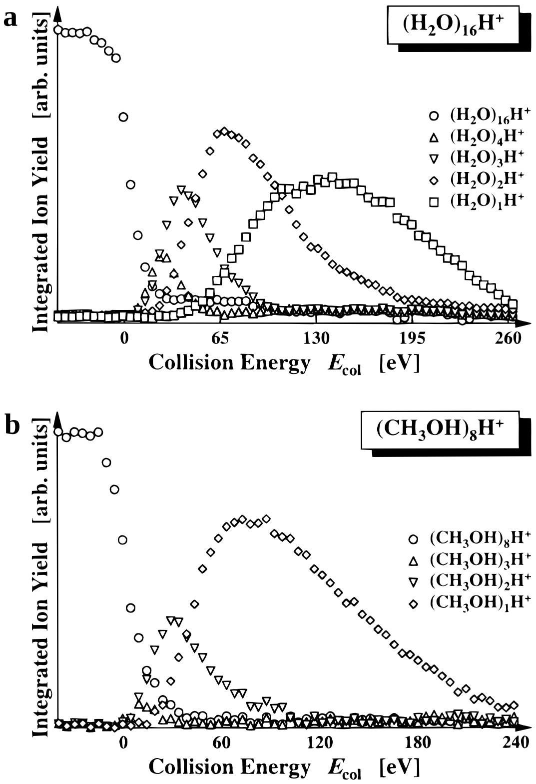

Figure 1. (a) Yield of charged cluster fragments due to the collision of protonated water cluster ions $(H_2O)_{16}H^+$ with a diamond target. The measured signal of scattered cluster ions is integrated for each mass and is plotted as a function of the collision energy E_{col}. Data points to the left of $E_{\text{col}} = 0$ eV represent reflected cluster ions. The relative energy spread of the incident cluster ions is less than 1% of the primary beam energy $E_{\text{i}} \simeq 1950$ eV. (b) Fragmentation pattern of protonated methanol cluster ions $(CH_3OH)_8H^+$ as a function of the collision energy.

d is the distance between the grounded mesh and the target surface (typically 2.0 mm), and m the mass of the fragment ion. Typical values are several tens of nanoseconds, which is considerably shorter than what is usually accessible by experiments using reflectrons.

This kind of fragmentation pattern is similar for other hydrogen-bonded cluster ions such as ammonia[45,58] and methanol; see Figure 1b. For the smaller $(CH_3OH)_8H^+$ clusters, fragment ions up to three monomers can be detected, reflecting the overall picture that the larger the parent cluster, the larger the fragments can be. But even for clusters of up to 64 molecules, the largest detected fragment ions consist of a maximum of six molecules only.

Thus the *shattering* of clusters upon surface impact appears to be very much different from the size distribution of cluster fragmentation induced by low-energy deposition, usually interpreted in the frame of the well-known evaporative ensemble model, which is dominated by the (sequential) loss of monomeric units.[117] The fragment size distribution explored in the present experiments covers the regime of multiple fragmentation events[118−123] up to complete disintegration.[124]

This sharp transition between mostly parents and mostly small(est) fragments as a function of impact energy has been predicted theoretically[125,126] and can be explained as due to the competition of two, exponentially rising, entropic effects. It essentially depends only on the multitude of possible isomers. In this theoretical approach there is one underlying assumption, namely, that there is a rather rapid thermalization of the translational degrees of freedom.[127] In other words, the

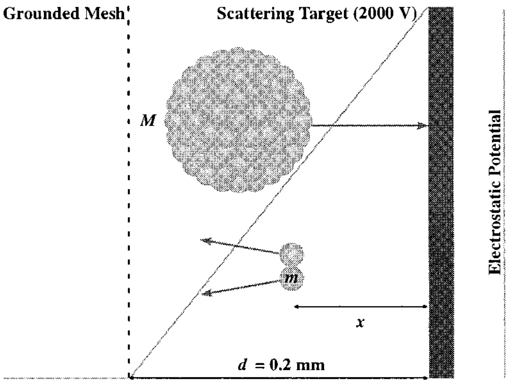

Figure 2. Schematic diagram illustrating the setup used for measuring the time scale of cluster fragmentation due to surface collision. It is based on the kinetic energy analysis of fragment ions.

experimental result of the pronounced transition to shattering can be explained by using thermodynamics.

Moreover, this theory suggests that the shattering is practically instantaneous (<1 ps) on impact. This prediction is investigated experimentally in the next section by placing an upper bound on the fragmentation time.

3.2. Time Scale of Cluster Fragmentation. The essential idea for the measurement of the fragmentation time scale of ion clusters upon surface impact is an energy analysis of the charged cluster fragments as shown in Figure 2 for the case of protonated ammonia cluster cations. Because the kinetic energy release during unimolecular decomposition of $(NH_3)_nH^+$ is in the order of only 10 meV,[128,129] any recoil energy of scattered fragment ions is neglected. If we assume a homogeneous electric field between the grounded mesh and the target surface, the kinetic energy E_{kin} of cluster fragment ions thus depends on where the fragmentation takes place:

$$E_{kin} = eU_{target}\left(\frac{xm}{dM} - \frac{x}{d} + 1\right)$$

x is the distance from the target where the fragmentation occurs, and M is the mass of the intact parent cluster ion.

The measurement in Figure 3a shows the result of a retarding field analysis of protonated ammonia fragment ions NH_4^+ for three different collision energies of the impacting $(NH_3)_2H^+$ ion. In all cases the mean kinetic energy of the fragment ions, resulting from the fit of an error function, is identical to the voltage applied to the target surface. The voltage resolution of 1 V corresponds to a spatial resolution of 200 nm, and the time to cover this distance is less than 120 ps.

Because this value is mainly limited by the voltage resolution, determined by comparing the high voltage applied at the target surface with the high voltage of the retarding field analyzer, this upper boundary can be improved by a simultaneous measurement of the kinetic energies of both the monomer and the dimer fragment ions of a larger cluster. As shown in Figure 3b for $(NH_3)_{10}H^+$ parent clusters, the mean kinetic energies of both fragment ions differ by less than 400 meV. Thus the time interval between the appearance of the dimer and the monomer fragment ions as the last (and slowest) step of the complete fragmentation process of a $(NH_3)_{10}H^+$ ion cluster is derived to be shorter than 80 ps.

This prompt shattering of cluster ions upon surface impact is faster than the well-known evaporation process, dominated by the (sequential) loss of monomeric units,[117] as has been shown by molecular dynamics simulations.[58] The metastable dissociation of protonated ammonia cluster ions can be expressed as

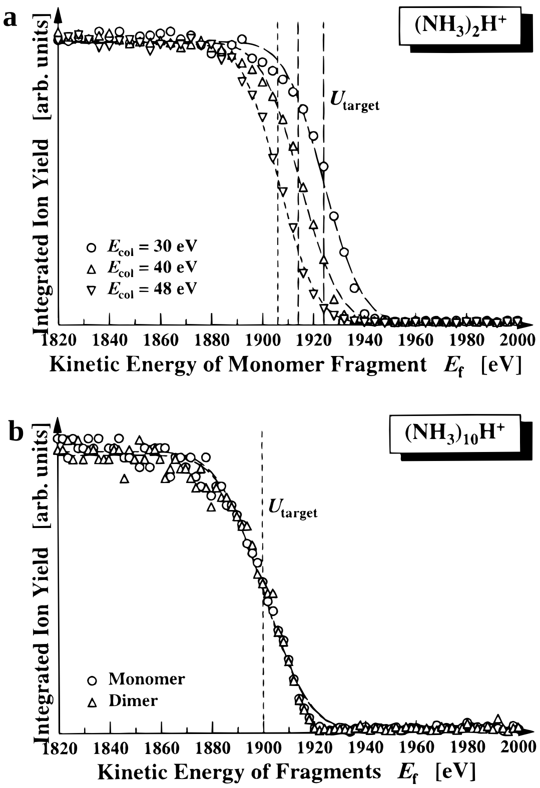

Figure 3. (a) Retarding field analysis of NH_4^+ cluster ion fragments, resulting from the impact of $(NH_3)_2H^+$ ions on the diamond target. Shown are three measurements for collision energies E_{col} = 30, 40, and 48 eV. The data points represent the integrated yield of NH_4^+ ions as a function of their kinetic energy as measured with the retarding field analyzer. The solid lines are fits of error functions to obtain the mean kinetic energy of the fragment ions. (b) Simultaneous retarding field analysis of monomer and dimer fragment ions resulting from the collision of $(NH_3)_{10}H^+$ cluster ions with a diamond target (E_{col} = 54 eV). Because both kinetic energies are derived from the same high voltage (of the retarding field analyzer), the accuracy can be higher by a factor of 2.5.

$$(NH_3)_nH^+ \rightarrow (NH_3)_{n-x}H^+ + x\,NH_3 \qquad x \geq 1$$

and has been determined to be in the microsecond domain.[129−131]

The reason why we pay special attention to this fast shattering is because this phenomenon provides evidence for the ultrafast dissipation and redistribution of energy in the impacting cluster. The implications for cluster impact chemistry are that this energy will be available to activate reactants in the cluster and also that the products of any chemical reaction will be kinetically stable because the cluster rapidly disintegrates after impact and thus is not able to confine or relax the products.

3.3. Collisional Energy Loss to the Target. Another important aspect toward the goal of energetically rich cluster reactants is the collisional energy loss of the impinging cluster ions to the target. This question can be solved by measuring the recoil energy of the intact scattered parent cluster ions. The recoil energy E_{rec} is given as the difference between the mean kinetic energy of scattered ions E_s and the target potential U_{target}: $E_{rec} = E_s - eU_{target}$.

Results for the elasticity ϵ as the ratio of the recoil energy E_{rec} to the impact energy E_{col} are presented in Figure 4 for protonated ammonia ion clusters $(NH_3)_nH^+$, n = 1, 2, 4, 5, 7, as a function of the impact energy E_{col}: For low impact energies

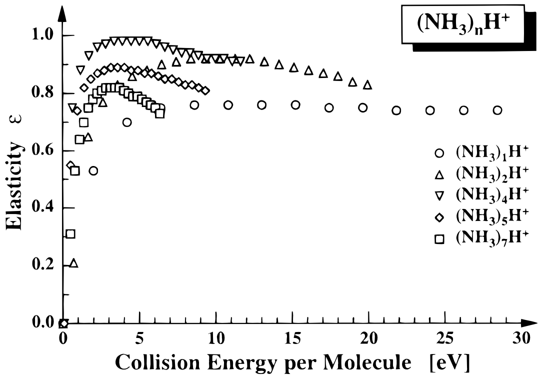

Figure 4. Collisional elasticity $\epsilon = E_{rec}/E_{col}$ for protonated ammonia cluster ions $(NH_3)_nH^+$ as a function of the collision energy E_{col}.

(<2.5 eV/molecule), cluster ions scattered off the target surface lost most of their initial kinetic energy, while for higher impact energies the elasticity of the cluster-surface collision is surprisingly high: Typically 75% of the impact kinetic energy is retained by the intact scattered parent cluster ions. Due to the stiff diamond surface, the small energy transfer to the target is not completely unexpected; it is compatible with the results of molecular dynamics calculations.[132−134]

Larger cluster ions are scattered less elastically and a large fraction of them shatter to smallest fragments. Because at higher collision energies most of the ion clusters are already shattered (see Figure 1), the large elasticity implies that the initial kinetic energy of the cluster ions is efficiently converted to internal excitations of the ion clusters: Once the clusters have acquired sufficient internal energy, they will shatter.[58]

3.4. Collision-Induced Dissociation. The results presented so far prove the fast and efficient fragmentation of ion clusters upon surface impact, the fast kinetic energy redistribution within the cluster ions, and the minor loss of kinetic energy to the target. Another indication for the high energy content within the cluster ions is the possibility of breaking *molecular* bonds. An example for the dissociation of toluene cluster ions upon surface impact is given in Figure 5.

Shown are secondary time-of-flight spectra of ions scattered off the target surface after the impact of toluene pentamer ions $(C_6H_6CH_2)_5^+$. For collision energies smaller $E_{col} \simeq 30$ eV some intact rebounding parent cluster ions and some dimer ions $(C_6H_6CH_2)_2^+$ as well as the toluene monomer ion can be detected. At collision energies between $E_{col} \simeq 16$ eV and $E_{col} \simeq 160$ eV the toluene monomer ion is the dominating mass peak, while for collision energies higher than $E_{col} \simeq 60$ eV the cluster ions start to dissociate. The most abundant dissociation product detected is $C_6H_i^+$, until at impact energies larger than $E_{col} \simeq 120$ eV the molecules dissociate completely and the whole $C_nH_i^+$ series evolves, $n = 2-6$.

3.5. Impact-Induced Chemical Reactions. While collision-induced dissociation reactions are well-known from individual molecule surface scattering, the most demanding challenge for cluster solid target collisions are cluster-specific, collective phenomena, such as the *formation* of chemical bonds.[135−141] The first example of a chemical reaction induced by clusters colliding with a solid surface is the reaction of iodomethane cluster anions $(CH_3I)_n^-$ to molecular iodine I_2^-. Figure 6 presents secondary time-of-flight spectra of $(CH_3I)_5^-$ cluster anions scattered off the diamond target surface for various impact energies: For very low collision energies $E_{col} < 20$ eV, besides the parent cluster ions, hydrogen anions H^-, atomic iodine I^- as well as a few iodomethane dimer ions $(CH_3I)_2^-$ can be observed. While the dimer anions gradually cease to exist for higher impact energies, a new peak due to molecular iodine I_2^- evolves for collision energies $E_{col} > 25$ eV. It reaches its maximum intensity at around $E_{col} = 200$ eV, where it saturates.

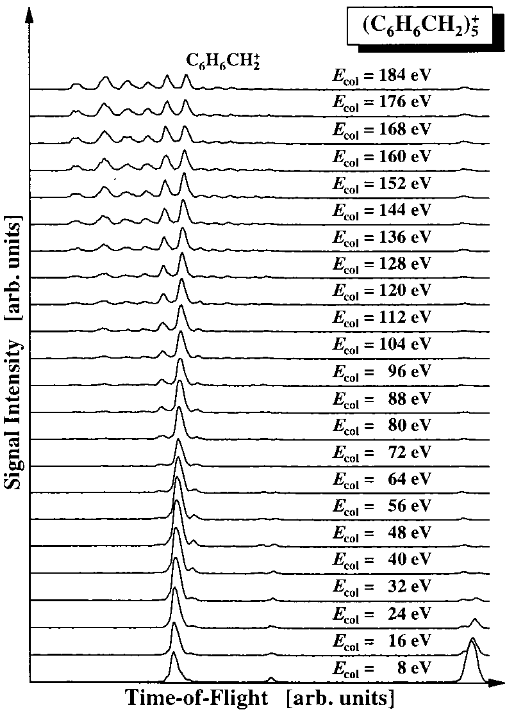

Figure 5. Secondary time-of-flight spectra of ions scattered off the diamond target surface after the impact of toluene cluster cations $(C_6H_6CH_2)_5^+$.

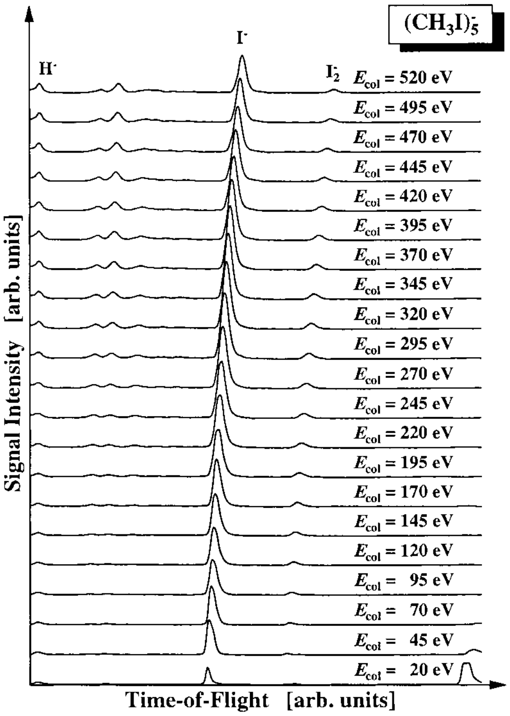

Figure 6. Secondary time-of-flight spectra of impacting iodomethane cluster anions $(CH_3I)_5^-$ for various collision energies E_{col}.

The cluster size dependence of the normalized reaction yield is shown in Figure 7 and can be best described by a fit of the functional form $I_2^-/I^- \propto \sqrt{n-1}$. Each data point represents at least three experimental measurements. The standard deviation of the reported values is in the range $1.5\sigma = 10\%$.

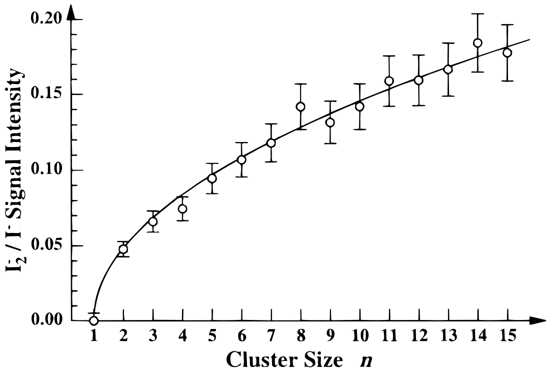

Figure 7. Reaction yield of molecular iodine I_2^- normalized to atomic iodine fragments I^- as a function of the size n of the impacting iodomethane cluster anions $(CH_3I)_n^-$. Both the reaction yield and the fragment ion signal are taken at the collision energy of the impacting cluster ions yielding the largest signal, typically at around $E_{col} = 200$ eV. The solid line is a fit to the data points, see text.

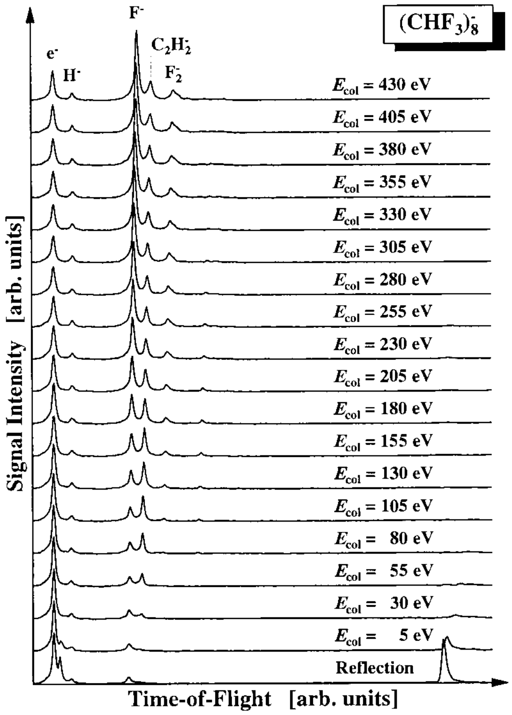

Figure 8. Secondary time-of-flight spectra of impacting trifluoromethane cluster anions $(CHF_3)_8^-$.

We would like to emphasize some important characteristics of the above results: The first one is the existence of an energy threshold of about 3 eV/molecule for the detection of the collision-induced reaction of the iodomethane pentamer anion to molecular iodine, depicted in Figure 6. The second aspect is the remarkable cluster size dependence of the reaction yield: While no reaction can be detected for the single molecular ion, the relative reaction yield rises constantly up to 15% for cluster ions consisting of 15 iodomethane molecules. Also, within the accuracy of the data, no effect due to the filling of the first solvation shell can be observed. Finally, the low flux of approximately 10^6 cluster ions per second impinging on the target surface should be mentioned: Even if we assume a sticking factor of 1, the probability for a significant contribution to the molecular bond formation via a recombinative desorption mechanism can be safely neglected.

To explore the effect of the solvent on the reactivity, trifluoromethane cluster anions $(CHF_3)_n^-$ have been investigated as well. Figure 8 presents secondary time-of-flight spectra due to the impact of $(CHF_3)_8^-$ cluster anions on the diamond target. For collision energies above $E_{col} \simeq 25$ eV $C_2H_2^-$ anions can be detected, which exhibit a maximum intensity for intermediate impact energies of about $E_{col} \simeq 150$ eV. This behavior is markedly different both from the observation of the F^- fragment ions as well as from the measurement of the F_2^- reaction product. In the latter cases the intensity grows steadily with increasing collision energy.

Finally the impact of difluorchloromethane cluster anions $(CHClF_2)_n^-$ has been measured to lead to fragment ions H^-, F^-, Cl^-, and the reaction product ions ClF^- as well as F_2^-.

4. Summary and Conclusions

We have presented experimental results showing that the scattering of molecular cluster ions from a solid surface can be almost elastic with only a minor energy loss to the target. In the particular case of protonated ammonia cluster cations $(NH_3)_nH^+$ impacting on a diamond-coated silicon target, typically 75% of the initial kinetic energy is retained by intact scattered cluster ions.

Once the impinging cluster ions have acquired sufficient internal energy, they will fragment, mostly to monomers. This pronounced transition from intact scattered cluster ions to their complete fragmentation as a function of the collision energy is very remarkable due to the absence of any fragments with intermediate sizes or sizes close to the original parent. This behavior seems to be quite general for hydrogen-bonded ion clusters.

The time needed for the complete fragmentation of a $(NH_3)_{10}H^+$ cluster ion upon surface impact is faster than 80 ps. According to molecular dynamics simulations,[58] this upper boundary actually can exclude a sequential loss process, such as metastable dissociation.

Due to this ultrafast energy distribution within the cluster ions, one can prepare “superheated” clusters with enough energy for breaking most or all intermolecular bonds. The technique of cluster impact opens a new energetic regime, allowing energy deposition of 1−50 eV/molecule on a femtosecond time scale.

This energy can be used to break and even to *form new molecular bonds*. Chemical reactions, induced by cluster impact, have been demonstrated with quite a large reaction yield. Even for the small $(CH_3I)_n^-$ cluster ions investigated so far ($n < 15$), a relative reaction yield of 15% I_2^- molecules per I^- fragment could be achieved. Similar reactions have been presented as well and lead us to conclude that cluster impact-induced chemical reactions might represent a new and quite general applicable mechanism of femtosecond chemistry.

Acknowledgment. This work would not have been possible without the skilfull support of the mechanical workshop, headed by N. Lavie. We acknowledge fruitful discussions with I. Becker, O. Chesnovsky, R. D. Levine, T. D. Märk, and T. Raz. This work was supported by a grant from GIF. W. Christen gratefully acknowledges a MINERVA fellowship.

References and Notes

(1) Even, U.; de Lange, P. J.; Jonkman, H. T.; Kommandeur, J. *Phys. Rev. Lett.* **1986**, *56*, 965.

(2) Vostrikov, A. A.; Dubov, D. Y. *Z. Phys. D* **1991**, *20*, 61.

(3) Holland, R. J.; Xu, G. Q.; Levkoff, J.; Robertson, A., Jr.; Bernasek, S. L. *J. Chem. Phys.* **1988**, *88*, 7952.

(4) Vostrikov, A. A.; Dubov, D. Y.; Predtechenskiy, M. R. *Chem. Phys. Lett.* **1987**, *139*, 124.

(5) Mironov, S. G.; Rebrov, A. K.; Semyachkin, B. E.; Vostrikov, A. A. *Surf. Sci.* **1981**, *106*, 212.

(6) Vostrikov, A. A.; Dubov, D. Y.; Gilyova, V. P. In *Symposium on Atomic and Surface Physics*, Märk, T. D.; Howorka, F., Eds.; Obertraun, Austria, 1990; pp 443−448.

(7) Vostrikov, A. A.; Dubov, D. Y. In *Rarefied Gas Dynamics*; Beylich, A. E., Ed.; VCH: Weinheim, Germany 1991; pp 1337−1344.

(8) Benslimane, M.; Châtelet, M.; De Martino, A.; Pradère, F.; Vach, H. *Chem. Phys. Lett.* **1995**, *237*, 323.

(9) Christen, W.; Kompa, K.-L.; Schröder, H.; Stülpnagel, H. *Ber. Bunsen-Ges. Phys. Chem.* **1992**, *96*, 1197.

(10) Châtelet, M.; De Martino, A.; Pettersson, J.; Pradère, F.; Vach, H. *Chem. Phys. Lett.* **1992**, *196*, 563.

(11) Vostrikov, A. A.; Dubov, D. Y.; Gilyova, V. P. *Prog. Astron. Aeronautics* **1989**, *117*, 335.

(12) Vostrikov, A. A.; Mironov, S. G.; Semyachkin, B. E. *Soviet Phys. Technol. Phys.* **1982**, *27*, 705.

(13) Tepper, G.; Miller, D. *Phys. Rev. Lett.* **1992**, *69*, 2927.

(14) Tepper, G.; Miller, D. *J. Chem. Phys.* **1993**, *98*, 9585.

(15) Christen, W. *Kurzzeitdynamik elektronischer Wechselwirkung von Molekülen und Clustern mit Festkörperoberflächen* Ph.D. Thesis, Ludwig-Maximilians-Universität, München, Germany, 1996.

(16) Vach, H.; De Martino, A.; Benslimane, M.; Châtelet, M.; Pradère, F. *J. Chem. Phys.* **1994**, *100*, 8526.

(17) Tepper, G.; Miller, D. *Surf. Sci.* **1994**, *312*, 310.

(18) Gspann, J.; Krieg, G. *J. Chem. Phys.* **1974**, *61*, 4037.

(19) Becker, E. W.; Klingelhöfer, R.; Mayer, H. *Z. Naturforsch. A* **1968**, *23*, 274.

(20) Vostrikov, A. A.; Dubov, D. Y.; Predtechenskii, M. R. *Soviet Phys. Technol. Phys.* **1988**, *33*, 1153.

(21) Vostrikov, A. A.; Dubov, D. Y.; Predtechenskii, M. R. *Soviet Phys. Technol. Phys.* **1987**, *32*, 459.

(22) De Lange, P. J.; Renkema, P. J.; Kommandeur, J. *J. Phys. Chem.* **1988**, *92*, 5749.

(23) Vostrikov, A. A.; Dubov, D. Y.; Predtechenskii, M. R. *Soviet Phys. Technol. Phys.* **1986**, *31*, 821.

(24) Châtelet, M.; Benslimane, M.; De Martino, A.; Pradère, F.; Vach, H. *Surf. Sci.* **1996**, *352−354*, 50.

(25) Menzel, C.; Knöner, A.; Kutzner, J.; Zacharias, H. *Z. Phys. D* **1996**, *38*, 179.

(26) De Martino, A.; Benslimane, M.; Châtelet, M.; Pradère, F.; Vach, H. *J. Chem. Phys.* **1996**, *105*, 7828.

(27) Pradère, F.; Benslimane, M.; Châtelet, M.; De Martino, A.; Vach, H. *Surf. Sci.* **1997**, *375*, L375.

(28) Andersson, P. U.; Tomsic, A.; Andersson, M. B.; Pettersson, J. B. C. *Chem. Phys. Lett.* **1997**, *279*, 100.

(29) Andersson, P. U.; Pettersson, J. B. C. *Z. Phys. D* **1997**, *41*, 57.

(30) Vostrikov, A. A.; Zadorozhny, A. M.; Dubov, D. Y.; Witt, G.; Kazakova, I. V.; Bragin, O. A.; Kazakov, V. G.; Kikhtenko, V. N.; Tyutin, A. A. *Z. Phys. D* **1997**, *40*, 542.

(31) Fort, E.; Pradère, F.; De Martino, A.; Vach, H.; Châtelet, M. *Eur. Phys. J. D* **1998**, *1*, 79.

(32) Shiromaru, H.; Moriwaki, T.; Kittaka, C.; Achiba, Y. *Z. Phys. D* **1991**, *20*, 141.

(33) St. John, P. M.; Whetten, R. L. *Chem. Phys. Lett.* **1992**, *196*, 330.

(34) Beck, R. D.; St. John, P.; Homer, M. L.; Whetten, R. L. *Chem. Phys. Lett.* **1991**, *187*, 122.

(35) Beck, R. D.; St. John, P.; Homer, M. L.; Whetten, R. L. *Science* **1991**, *253*, 879.

(36) Whetten, R. L.; Homer, M. L.; Li, X.; Livingston, F. E.; St. John, P. M.; Beck, R. D. *Ber. Bunsen-Ges. Phys. Chem.* **1992**, *96*, 1120.

(37) St. John, P. M.; Beck, R. D.; Whetten, R. L. *Phys. Rev. Lett.* **1992**, *69*, 1467.

(38) St. John, P. M.; Beck, R. D.; Whetten, R. L. *Z. Phys. D* **1993**, *26*, 226.

(39) Yeretzian, C.; Beck, R. D.; Whetten, R. L. *Int. J. Mass Spectrom. Ion Proc.* **1994**, *135*, 79.

(40) Whetten, R. L.; Yeretzian, C.; St. John, P. M. *Int. J. Mass Spectrom. Ion Proc.* **1994**, *138*, 63.

(41) Moriwaki, T.; Matsuura, H.; Aihara, K.; Shiromaru, H.; Achiba, Y. *J. Phys. Chem.* **1992**, *96*, 9092.

(42) St. John, P. M.; Yeretzian, C.; Whetten, R. L. *J. Phys. Chem.* **1992**, *96*, 9100.

(43) Whetten, R. L. *Acc. Chem. Res.* **1993**, *26*, 49.

(44) Tsukuda, T.; Yasumatsu, H.; Sugai, T.; Terasaki, A.; Nagata, T.; Kondow, T. *J. Phys. Chem.* **1995**, *99*, 6367.

(45) Hendell, E.; Even, U.; Raz, T.; Levine, R. D. *Phys. Rev. Lett.* **1995**, *75*, 2670.

(46) Yasumatsu, H.; Tsukuda, T.; Sugai, T.; Terasaki, A.; Nagata, T.; Kondow, T. *Surf. Rev. Lett.* **1996**, *3*, 901.

(47) Tsukuda, T.; Yasumatsu, H.; Sugai, T.; Terasaki, A.; Nagata, T.; Kondow, T. *Surf. Rev. Lett.* **1996**, *3*, 875.

(48) Kawada, Y.; Shiromaru, H.; Moriwaki, T.; Achiba, Y. *Surf. Rev. Lett.* **1996**, *3*, 869.

(49) Kondow, T. *Surf. Rev. Lett.* **1996**, *3*, 631.

(50) Terasaki, A.; Tsukuda, T.; Yasumatsu, H.; Sugai, T.; Kondow, T. *Surf. Rev. Lett.* **1996**, *3*, 591.

(51) Terasaki, A.; Tsukuda, T.; Yasumatsu, H.; Sugai, T.; Kondow, T. *J. Chem. Phys.* **1996**, *104*, 1387.

(52) Moriwaki, T.; Shiromaru, H.; Achiba, Y. *Z. Phys. D* **1996**, *37*, 169.

(53) Yasumatsu, H.; Koizumi, S.; Terasaki, A.; Kondow, T. *J. Chem. Phys.* **1996**, *105*, 9509.

(54) Terasaki, A.; Yamaguchi, H.; Yasumatsu, H.; Kondow, T. *Chem. Phys. Lett.* **1996**, *262*, 269.

(55) Yasumatsu, H.; Terasaki, A.; Kondow, T. *J. Chem. Phys.* **1997**, *106*, 3806.

(56) Kaiser, B.; Bernhardt, T. M.; Rademann, K. *Nucl. Instrum. Methods Phys. Res. B* **1997**, *125*, 223.

(57) Bernhardt, T. M.; Kaiser, B.; Rademann, K. *Z. Phys. D* **1997**, *40*, 327.

(58) Christen, W.; Even, U.; Raz, T.; Levine, R. D. *Int. J. Mass Spectrom. Ion Proc.* **1998**, *174*, 35.

(59) Christen, W.; Even, U.; Raz, T.; Levine, R. D. *J. Chem. Phys.* **1998**, *108*, 10262.

(60) Yasumatsu, H.; Terasakia, A.; Kondow, T. *Int. J. Mass Spectrom. Ion Proc.* **1998**, *174*, 297.

(61) Beuhler, R. J.; Friedman, L. *Nucl. Instrum. Methods* **1980**, *170*, 309.

(62) Gall, L. N.; Krasnov, N. V.; Lokhin, L. R.; Muradymov, M. Z. In *Rarefied Gas Dynamics*; Beylich, A. E., Ed.; VCH: Weinheim, Germany, 1991; pp 1175−1178.

(63) Töglhofer, K.; Aumayr, F.; Kurz, H.; Winter, H.; Scheier, P.; Märk, T. D. *Europhys. Lett.* **1993**, *22*, 597.

(64) Töglhofer, K.; Aumayr, F.; Kurz, H.; Winter, H.; Scheier, P.; Märk, T. D. *J. Chem. Phys.* **1993**, *99*, 8254.

(65) Haberland, H.; Winterer, M. *Rev. Sci. Instrum.* **1983**, *54*, 764.

(66) Staudenmaier, G.; Hofer, W. O.; Liebl, H. *Int. J. Mass Spectrom. Ion Phys.* **1976**, *21*, 103.

(67) Töglhofer, K.; Aumayr, F.; Kurz, H.; Winter, H.; Scheier, P.; Märk, T. D. *Nucl. Instrum. Methods Phys. Res. B* **1994**, *88*, 44.

(68) Mahoney, J. F.; Parilis, E. S.; Perel, J.; Ruatta, S. A. *Nucl. Instrum. Methods Phys. Res. B* **1993**, *73*, 29.

(69) Beuhler, R. J. *J. Appl. Phys.* **1983**, *54*, 4118.

(70) Chanut, Y.; Martin, J.; Salin, R.; Moser, H. O. *Surf. Sci.* **1981**, *106*, 563.

(71) Thum, F.; Hofer, W. O. *Surf. Sci.* **1979**, *90*, 331.

(72) Hendell, E.; Even, U. *J. Chem. Phys.* **1995**, *103*, 9045.

(73) Baudin, K.; Brunelle, A.; Della-Negra, S.; Depauw, J.; Le Beyec, Y.; Parilis, E. S. *Nucl. Instrum. Methods Phys. Res. B* **1996**, *117*, 47.

(74) Billebaud, A.; Dauvergne, D.; Fallavier, M.; Kirsch, R.; Poizat, J.-C.; Remillieux, J.; Rothard, H.; Thomas, J.-P. *Nucl. Instrum. Methods Phys. Res. B* **1996**, *112*, 79.

(75) Aumayr, F.; Vana, M.; Winter, H.; Drexel, H.; Grill, V.; Senn, G.; Matt, S.; Scheier, P.; Märk, T. D. *Int. J. Mass Spectrom. Ion Proc.* **1997**, *163*, 9L.

(76) Winter, H.; Vana, M.; Betz, G.; Aumayr, F.; Drexel, H.; Scheier, P.; Märk, T. D. *Phys. Rev. A* **1997**, *56*, 3007.

(77) Aumayr, F.; Betz, G.; Märk, T. D.; Scheier, P.; Winter, H. P. *Int. J. Mass Spectrom. Ion Proc.* **1998**, *174*, 317.

(78) Susuki, Y. *Z. Phys. D* **1997**, *42*, 293.

(79) Busmann, H.-G.; Lill, T.; Reif, B.; Hertel, I. V. *Surf. Sci.* **1992**, *272*, 146.

(80) Busmann, H.-G.; Lill, T.; Hertel, I. V. *Chem. Phys. Lett.* **1991**, *187*, 459.

(81) Busmann, H.-G.; Lill, T.; Reif, B.; Hertel, I. V.; Maguire, H. G. *J. Chem. Phys.* **1993**, *98*, 7574.

(82) Yeretzian, C.; Hansen, K.; Beck, R. D.; Whetten, R. L. *J. Chem. Phys.* **1993**, *98*, 7480.

(83) Lill, T.; Busmann, H.-G.; Reif, B.; Hertel, I. V. *Surf. Sci.* **1994**, *312*, 124.

(84) Weis, P.; Beck, R. D.; Bräuchle, G.; Kappes, M. M. *J. Chem. Phys.* **1994**, *100*, 5684.

(85) Yeretzian, C.; Whetten, R. L. *Z. Phys. D* **1992**, *24*, 199.

(86) Lill, T.; Busmann, H.-G.; Reif, B.; Hertel, I. V. *Appl. Phys. A* **1992**, *55*, 461.

(87) Hamza, A. V.; Balooch, M.; Moalem, M.; Olander, D. R. *Chem. Phys. Lett.* **1994**, *228*, 117.

(88) Beck, R. D.; St. John, P.; Alvarez, M. M.; Diederich, F.; Whetten, R. L. *J. Phys. Chem.* **1991**, *95*, 8402.

(89) Moalem, M.; Balooch, M.; Hamza, A. V.; Siekhaus, W. J.; Olander, D. R. *J. Chem. Phys.* **1993**, *99*, 4855.

(90) Yeretzian, C.; Hansen, K.; Alvarez, M. M.; Min, K. S.; Gillan, E. G.; Holczer, K.; Kaner, R. B.; Whetten, R. L. *Chem. Phys. Lett.* **1992**, *196*, 337.

(91) Yeretzian, C.; Hansen, K.; Diederich, F.; Whetten, R. L. *Z. Phys. D* **1993**, *26*, 300 (suppl).

(92) Yeretzian, C.; Hansen, K.; Whetten, R. L. *Science* **1993**, *260*, 652.

(93) Yeretzian, C.; Hansen, K.; Diederich, F.; Whetten, R. L. *Nature (London)* **1992**, *353*, 44.

(94) Lill, T.; Busmann, H.-G.; Hertel, I. V. *Z. Phys. B* **1993**, *91*, 267.

(95) Whetten, R. L.; Yeretzian, C. *Int. J. Modern Phys. B* **1992**, *6*, 3801.

(96) Lill, T.; Busmann, H.-G.; Lacher, F.; Hertel, I. V. *Chem. Phys.* **1995**, *193*, 199.

(97) Lill, T.; Lacher, F.; Busmann, H.-G.; Hertel, I. V. *Phys. Rev. Lett.* **1993**, *71*, 3383.

(98) Beck, R. D.; Weis, P.; Rockenberger, J.; Michel, R.; Fuchs, D.; Benz, M.; Kappes, M. M. *Surf. Rev. Lett.* **1996**, *3*, 881.

(99) Beck, R. D.; Weis, P.; Rockenberger, J.; Kappes, M. M. *Surf. Rev. Lett.* **1996**, *3*, 771.

(100) Weis, P.; Rockenberger, J.; Beck, R. D.; Kappes, M. M. *J. Chem. Phys.* **1996**, *104*, 3629.

(101) Beck, R. D.; Rockenberger, J.; Weis, P.; Kappes, M. M. *J. Chem. Phys.* **1996**, *104*, 3638.

(102) Campbell, E. E. B.; Hertel, I. V. *Nucl. Instrum. Methods Phys. Res. B* **1996**, *112*, 48.

(103) Beck, R. D.; Warth, C.; May, K.; Kappes, M. M. *Chem. Phys. Lett.* **1996**, *257*, 557.

(104) Tsipinyuk, B.; Budrevich, A.; Grinberg, M.; Kolodney, E. *J. Chem. Phys.* **1997**, *106*, 2449.

(105) Budrevich, A.; Tsipinyuk, B.; Bekkerman, A.; Kolodney, E. *J. Chem. Phys.* **1997**, *106*, 5771.

(106) Beck, R. D.; Weis, P.; Bräuchle, G.; Rockenberger, J. *Rev. Sci. Instrum.* **1995**, *66*, 4188.

(107) Kolodney, E.; Tsipinyuk, B.; Bekkerman, A.; Budrevich, A. *Nucl. Instrum. Methods Phys. Res. B* **1997**, *125*, 170.

(108) Beck, R. D.; Weis, P.; Bräuchle, G.; Kappes, M. M. *J. Chem. Phys.* **1994**, *100*, 262.

(109) Bekkerman, A.; Tsipinyuk, B.; Budrevich, A.; Kolodney, E. *Int. J. Mass Spectrom. Ion Proc.* **1997**, *167/168*, 559.

(110) Bekkerman, A.; Tsipinyuk, B.; Budrevich, A.; Kolodney, E. *Isr. J. Chem.* **1997**, *37*, 405.

(111) General Vacuum Inc., P. O. Box 605204, Cleveland, OH 44105.

(112) Dahl, D. A. *SIMION 3D*; Princeton Electronic Systems, Inc., P. O. Box 8627, Princeton, NJ 08543-8627; 1995.

(113) Xu, G.-Q.; Holland, R. J.; Bernasek, S. L.; Tully, J. C. *J. Chem. Phys.* **1989**, *90*, 3831.

(114) Xu, G.-Q.; Bernasek, S. L.; Tully, J. C. *J. Chem. Phys.* **1988**, *88*, 3376.

(115) Pettersson, J. B. C.; Marković, N. *Chem. Phys. Lett.* **1993**, *201*, 421.

(116) Marković, N.; Pettersson, J. B. C. *J. Chem. Phys.* **1994**, *100*, 3911.

(117) Klots, C. E. *J. Phys. Chem.* **1988**, *92*, 5864.

(118) Farizon, B.; Farizon, M.; Gaillard, M. J.; Genre, R.; Louc, S.; Martin, J.; Buchet, J. P.; Carré, M.; Senn, G.; Scheier, P.; Märk, T. D. *Int. J. Mass Spectrom. Ion Proc.* **1997**, *164*, 225.

(119) Ehlich, R.; Westerburg, M.; Campbell, E. E. B. *J. Chem. Phys.* **1996**, *104*, 1900.

(120) Ouaskit, S.; Farizon, B.; Farizon, M.; Gaillard, M. J.; Chevarier, A.; Chevarier, N.; Gerlic, E.; Stern, M. *Int. J. Mass Spectrom. Ion Proc.* **1994**, *139*, 141.

(121) LeBrun, T.; Berry, H. G.; Cheng, S.; Dunford, R. W.; Esbensen, H.; Gemmell, D. S.; Kanter, E. P.; Bauer, W. *Phys. Rev. Lett.* **1994**, *72*, 3965.

(122) Farizon, B.; Farizon, M.; Gaillard, M. J.; Gerlic, E.; Ouaskit, S. *Nucl. Instrum. Methods Phys. Res. B* **1994**, *88*, 86.

(123) Hvelplund, P.; Andersen, L. H.; Haugen, H. K.; Lindhard, J.; Lorents, D. C.; Malhotra, R.; Ruoff, R. *Phys. Rev. Lett.* **1992**, *69*, 1915.

(124) Mazuy, B.; Belkacem, A.; Chevallier, M.; Gaillard, M. J.; Poizat, J. C.; Remillieux, J. *Nucl. Instrum. Methods Phys. Res. B* **1987**, *28*, 497.

(125) Raz, T.; Even, U.; Levine, R. D. *J. Chem. Phys.* **1995**, *103*, 5394.

(126) Raz, T.; Levine, R. D. *J. Chem. Phys.* **1996**, *105*, 8097.

(127) Raz, T.; Levine, R. D. *Chem. Phys.* **1996**, *213*, 263.

(128) Lifshitz, C.; Louage, F. *J. Phys. Chem.* **1989**, *93*, 5633.

(129) Wei, S.; Tzeng, W. B.; Castleman, A. W., Jr. *J. Chem. Phys.* **1990**, *92*, 332.

(130) Echt, O.; Dao, P. D.; Morgan, S.; Castleman, A. W., Jr. *J. Chem. Phys.* **1985**, *82*, 4076.

(131) Wei, S.; Tzeng, W. B.; Castleman, A. W., Jr. *J. Chem. Phys.* **1990**, *93*, 2506.

(132) Cleveland, C. L.; Landman, U. *Science* **1992**, *257*, 355.

(133) Schek, I.; Raz, T.; Levine, R. D.; Jortner, J. *J. Chem. Phys.* **1994**, *101*, 8596.

(134) Raz, T.; Schek, I.; Ben-Nun, M.; Even, U.; Jortner, J.; Levine, R. D. *J. Chem. Phys.* **1994**, *101*, 8606.

(135) Raz, T.; Levine, R. D. *Chem. Phys. Lett.* **1994**, *226*, 47.

(136) Raz, T.; Levine, R. D. *J. Am. Chem. Soc.* **1994**, *116*, 11167.

(137) Raz, T.; Levine, R. D. *J. Phys. Chem.* **1995**, *99*, 13713.

(138) Raz, T.; Levine, R. D. *J. Phys. Chem.* **1995**, *99*, 7495.

(139) Raz, T.; Levine, R. D. *Chem. Phys. Lett.* **1995**, *246*, 405.

(140) Gupta, M.; Walters, E. A.; Blais, N. C. *J. Chem. Phys.* **1996**, *104*, 100.

(141) Qi, L.; Sinnott, S. B. *J. Phys. Chem. B* **1997**, *101*, 6883.